



**HAL**  
open science

# A High-Resolution Belemnite Geochemical Analysis of Early Cretaceous (Valanginian-Hauterivian) Environmental and Climatic Perturbations

Gregory Price, Nico M M Janssen, Mathieu Martinez, Miguel Company,  
Justin H Vandavelde, Stephen T Grimes

► **To cite this version:**

Gregory Price, Nico M M Janssen, Mathieu Martinez, Miguel Company, Justin H Vandavelde, et al..  
A High-Resolution Belemnite Geochemical Analysis of Early Cretaceous (Valanginian-Hauterivian)  
Environmental and Climatic Perturbations. *Geochemistry, Geophysics, Geosystems*, 2018, 19 (10),  
pp.3832-3843. 10.1029/2018GC007676 . insu-02438978

**HAL Id: insu-02438978**

**<https://insu.hal.science/insu-02438978>**

Submitted on 14 Jan 2020

**HAL** is a multi-disciplinary open access archive for the deposit and dissemination of scientific research documents, whether they are published or not. The documents may come from teaching and research institutions in France or abroad, or from public or private research centers.

L'archive ouverte pluridisciplinaire **HAL**, est destinée au dépôt et à la diffusion de documents scientifiques de niveau recherche, publiés ou non, émanant des établissements d'enseignement et de recherche français ou étrangers, des laboratoires publics ou privés.

## RESEARCH ARTICLE

10.1029/2018GC007676

## Key Points:

- A high-resolution carbon and oxygen isotope record for the Early Cretaceous
- A robust characterization of Valanginian temperature evolution
- Carbonate oxygen isotope signal is primarily driven by seawater oxygen isotope changes and not temperature

## Supporting Information:

- Supporting Information S1
- Table S1
- Table S2

## Correspondence to:

G. D. Price,  
g.price@plymouth.ac.uk

## Citation:

Price, G. D., Janssen, N. M. M., Martinez, M., Company, M., Vandeveld, J. H., & Grimes, S. T. (2018). A high-resolution belemnite geochemical analysis of Early Cretaceous (Valanginian-Hauterivian) environmental and climatic perturbations. *Geochemistry, Geophysics, Geosystems*, 19, 3832–3843. <https://doi.org/10.1029/2018GC007676>

Received 14 JUN 2018

Accepted 30 SEP 2018

Accepted article online 8 OCT 2018

Published online 18 OCT 2018

©2018. The Authors.

This is an open access article under the terms of the Creative Commons Attribution License, which permits use, distribution and reproduction in any medium, provided the original work is properly cited.

# A High-Resolution Belemnite Geochemical Analysis of Early Cretaceous (Valanginian-Hauterivian) Environmental and Climatic Perturbations

Gregory D. Price<sup>1</sup> , Nico M. M. Janssen<sup>2</sup>, Mathieu Martinez<sup>3</sup> , Miguel Company<sup>4</sup>, Justin H. Vandeveld<sup>1</sup> , and Stephen T. Grimes<sup>1</sup>

<sup>1</sup>School of Geography, Earth and Environmental Sciences, University of Plymouth, Plymouth, UK, <sup>2</sup>Waalstraat 156A, NL-3522 SV Utrecht, the Netherlands, <sup>3</sup>Géosciences Rennes, University of Rennes, Rennes, France, <sup>4</sup>Departamento de Estratigrafía y Paleontología Facultad de Ciencias, Universidad de Granada, Granada, Spain

**Abstract** The Early Cretaceous Weissert event, characterized by a positive carbon isotope excursion and coincident with the Paraná-Etendeka volcanism, saw a biogeochemical chain of events that ultimately led to an increase in carbon burial. A conclusive link between the Paraná-Etendeka volcanism and its impact upon the environment remains, however, elusive. Here we reconstruct temperature through the Weissert event from Mg/Ca ratios of belemnites from the Vocontian Trough (France) and SE Spain and use carbon isotopes to link our temperature reconstruction to marine records of carbon cycling. We provide evidence that the Paraná-Etendeka volcanism, unlike some large igneous provinces, did not cause a climate warming. The case can be made for cooling in the last stages of the Weissert event, which possibly reflects substantial CO<sub>2</sub> drawdown. In the absence of warming and consequent accelerated hydrological cycling and the relatively long duration of the eruptive phase of the Paraná-Etendeka, an alternate trigger for increased fertilization of the oceans is implicated.

## 1. Introduction

The Early Cretaceous Weissert event, characterized by a positive carbon isotope excursion, coincides with an increase in atmospheric CO<sub>2</sub>, a demise of shallow-water carbonate platforms (Föllmi et al., 2006), and biocalcification crisis (Barbarin et al., 2012). The origin of the Weissert event has been the subject of much debate whereby Lini et al. (1992), Gröcke et al. (2005), Erba et al. (2004), and Duchamp-Alphonse et al. (2007) have speculated that an increase in atmospheric CO<sub>2</sub> and environmental changes are linked to volcanism associated with the Paraná-Etendeka igneous province. Although links between other large igneous provinces (LIPs) and warming events have been established (e.g., Kerr, 1998; Tejada et al., 2009), this is not the case for the Paraná-Etendeka igneous province (e.g., Bodin et al., 2015; Dodd et al., 2015). Following the positive carbon isotope excursion of the Weissert event, subsequent organic-carbon storage has been considered to have triggered a decline in atmospheric pCO<sub>2</sub>. Many studies (e.g., McArthur et al., 2004, 2007; Meissner et al., 2015; Price & Passey, 2013; Pucéat et al., 2003; van de Schootbrugge et al., 2000) do indeed propose cooling in the late Valanginian (coincident with the most positive carbon isotopes values), based on oxygen-isotope records derived from belemnites and fish tooth enamels. In response to a period of global cooling, McArthur et al. (2007) propose also the formation of a substantial amount of polar ice. The occurrence of glendonites and dropstones (Kemper, 1987; Price, 1999) and changes in calcareous nannofossils (Melinte & Mutterlose, 2001) also appear to confirm cold conditions during the Valanginian. Despite these numerous studies, a robust picture of Valanginian temperature evolution has yet to be fully developed. Here we evaluate high-resolution temporal trends through the Early Cretaceous (Valanginian-Hauterivian) of oxygen isotopes and Mg/Ca ratios of belemnites from the Vocontian Trough (France) and SE Spain in order to develop a robust view of the evolution of temperature. The analysis of carbon isotopes permits the comparison of paleotemperatures with changes in carbon cycling.

## 2. Geologic Setting

### 2.1. The Vocontian Trough, France

The sections in the Vocontian Trough (Figure 1b) have been extensively described by Reboulet et al. (1992) and Bulot et al. (1993) among others. They consist of hemipelagic marl-limestone alternations, allowing

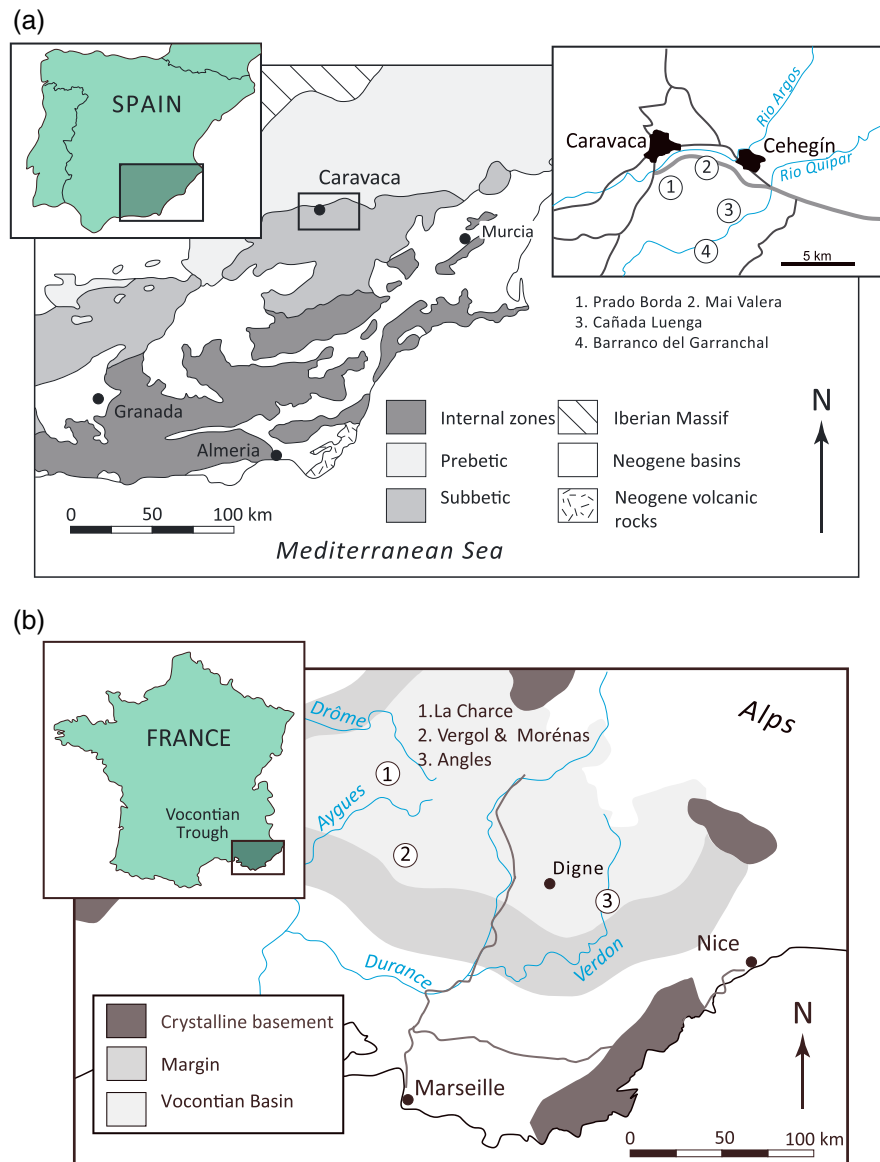


**Figure 1.** Location of (a) Spanish (modified from Aguado et al., 2000; Martinez et al., 2012) and (b) French (modified from Reboulet & Atrops, 1997; Gréselle & Pittet, 2010) sections and location of the sections studied.

bed-to-bed correlations between sections (Cotillon et al., 1980). The sediments are well constrained in terms of ammonite (Bulot et al., 1993; Reboulet & Atrops, 1997) and nannofossil (Barbarin et al., 2012; Duchamp-Alphonse et al., 2007; Gardin, 2008; Gréselle et al., 2011) biostratigraphy and comprise cyclic calcareous beds and darker gray, marly interbeds, with minor slumps intercalated in parts of some sections (Cotillon et al., 1980; Reboulet et al., 2003; Reboulet & Atrops, 1997). According to Huang et al. (1993), Giraud et al. (1995), and Martinez et al. (2015) the alternating lithologies show Milankovitch cyclicity, with sedimentation rates mostly being between 2 and 5 cm/ka.

During Berriasian to Hauterivian times, the sediments of the Vocontian Trough were deposited in the western region of the Tethyan Ocean (Figure 2) at a paleolatitude of 25–30°N (Masse et al., 1993; Figure 2). During much of Berriasian time, connection was weak or nonexistent between the Tethyan Realm of southern Europe and the more northerly Boreal Realm. Connection was more open from Valanginian times onward (e.g., Mutterlose, 1992), enabling widespread faunal exchange, either as a result of higher sea level at those times (Mutterlose, 1992) or combined with changing climate (Reboulet & Atrops, 1995).

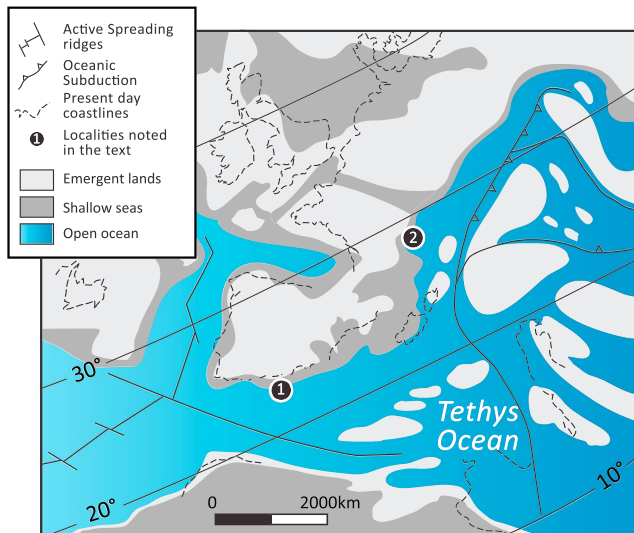


**Figure 2.** Early Cretaceous paleogeographic map modified from Masse et al. (1993).

## 2.2. The Subbetic Domain, Southeastern Spain, Betic Cordillera

The Cretaceous successions, located near Caravaca de la Cruz (Murcia Province; Figure 1a), consist of nodular limestones with abundant crinoid fragments, overlain by hemipelagic marl-limestone alternations (Aguado et al., 2000; Company & Tavera, 1982). Limestone bed thickness varies from one to several decimeters, while interbed thickness can occasionally reach 1 m. The succession is thought to have been deposited in a low-energy marine basinal setting, with an estimated water depth of a few hundreds of meters (Hoedemaeker & Leereveld, 1995; Janssen, 2003). For the Berriasian part of the section, the marl-limestone alternations have been attributed to orbital forcing (Sprenger & Ten Kate, 1993). This interpretation has been extended to the Hauterivian (e.g., Martinez et al., 2012). The limestone beds typically contain nannofossils, including coccolithophorids and nannoconus tests. Macrofauna consist largely of belemnite rostra (e.g., Janssen, 1997, 2003) and well-preserved ammonites, allowing detailed biostratigraphic zonation and correlation of the sections (Aguado et al., 2000; Company et al., 2003; Company & Tavera, 1982, 2015; Hoedemaeker & Leereveld, 1995).

During the Valanginian-Hauterivian interval the Subbetic domain was situated on the southern margin of the Iberian plate in the western region of the Tethys Ocean, at a low latitude between 20° and 25°N (Masse et al., 1993; Figure 2). From the Latest Jurassic to the Early Cretaceous, it was a passive margin, with thick hemipelagic postrift sedimentation smothering the submarine relief (Martín-Algarra et al., 1992).

## 3. Materials and Methods

The sections studied in Spain, located near Caravaca and Cehegín, are as follows: Prado Borda section, 2.1 km SSE of Caravaca (38°05′13″N 1°51′14″W); sections on the northeastern slope of Mai Valera Mountain, 2 km west of Cehegín (38°05′39″N 1°49′09″W); sections along the Cañada Luenga ravine, 3.1 km SSW of Cehegín (38°04′02″N 1°48′49″W); and the Barranco del Garranchal section, 5.5 km SSW of Cehegín (38°02′42″N 1°49′20″W). The sections studied in France are the La Charce section (44°28′09″N 5°26′37″W), an expanded, well-documented section that is the currently suggested Global Boundary Stratotype Section and Point (GSSP) candidate for the base of the Hauterivian Stage (Gradstein et al., 2012); the Vergol/Morénas section (a Berriasian/Valanginian GSSP candidate; Gradstein et al., 2012, 44°12′12″N 5°25′09″W); and the Angles section (the Valanginian Hypostratotype, 43°56′28″N 6°32′32″W). Belemnite samples from each section were collected bed by bed, and whenever possible, multiple samples were collected from each bed. In total, 136 belemnites from France have been analyzed, of which 35 of these are excluded due to potential diagenesis (see below) and are combined with a further 226 published analyses (from Bodin et al., 2015; Li et al., 2013; McArthur et al., 2007; van de Schootbrugge et al., 2000). In total, 124 belemnites from Spain have been analyzed in this study, of which 9 of these are excluded due to potential diagenesis and are combined with a further 18 published analyses (from McArthur et al., 2007). In order to accommodate these published isotopic data and isotopic data derived from different sections, data are plotted as numerical ages based on the ages of Tethyan ammonite zones/subzones from Reboulet et al. (2014) in Martinez et al. (2015). Ages are determined according to position of each sample within each ammonite zone/subzone, assuming a constant sedimentation rate. Adjustments for a variable sedimentation rate are made with respect to different thickness of each ammonite zone/subzone at each section examined.

The preservation of the belemnite rostra was assessed using cathodoluminescence (Figure 3) using an MK5 CITL instrument and trace element analysis (Ca, Sr, Mg, Fe, and Mn concentrations). The belemnites were prepared for stable isotope and trace element analysis by first removing the areas of the rostrum typically most prone to diagenesis (the rostrum exterior, apical region, alveolus, and observable cracks/fractures; e.g., McArthur et al., 2007; Meissner et al., 2015). The remaining calcite was then fragmented, washed in ultrapure (Type 1) water, and dried in a clean environment. Using 300 to 400 µg of carbonate, stable isotope data were generated on a VG Optima mass spectrometer with a Gilson autosampler at the University of Plymouth.

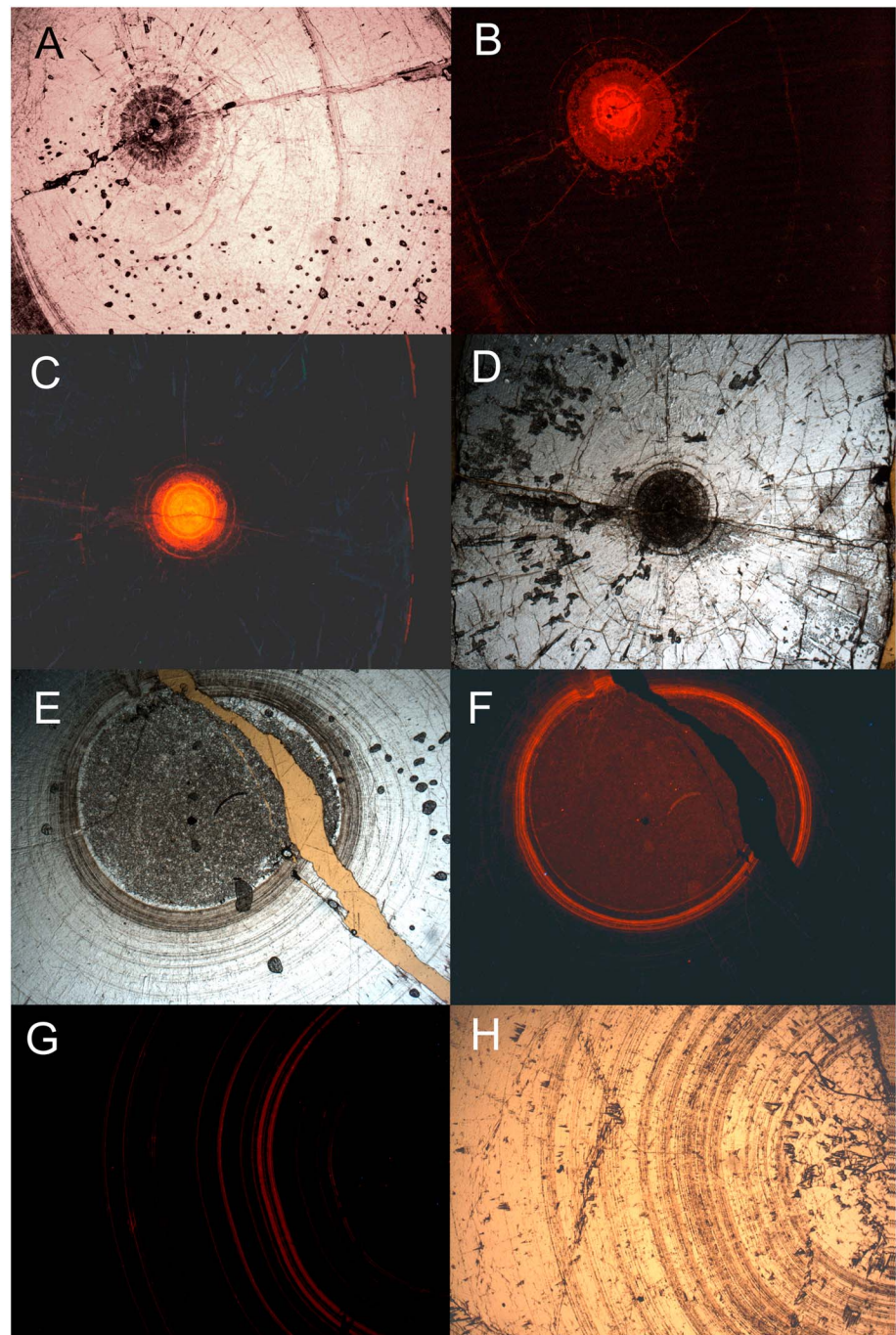


**Figure 3.** Photomicrographs (a) PPI and (b) cathodoluminescence (CL) of nonluminescent rostrum of *Duvalia*, Morénas section, with luminescent apical line area (Sample MYR001), Peregrinus Zone. Photomicrographs (c) CL and (d) PPI of nonluminescent rostrum of *Duvalia*, La Charce section, with luminescent apical line area (Sample LCY013), Peregrinus Zone. Photomicrographs (e) PPI and (f) CL of nonluminescent rostrum of *Hibolithes*, Morénas section with luminescent margin of the rostrum and sediment infill of conical cavity where phragmocone used to be (Sample MYR082), Inostranzewi (Campylotoxus) Zone. Photomicrographs (g) CL and (h) PPI of the rostrum of *Hibolithes cf. jaculoides* showing thin luminescent growth lines close to the apical line area from the Mai Valera section (Sample YP14–016), Inostranzewi Zone. PPI = Plane Polarized Light.

Isotope ratios were calibrated using standards of National Bureau of Standards and were given in  $\delta$  notation relative to the Vienna Pee Dee Belemnite (V-PDB). Reproducibility was generally better than 0.1‰ for samples and standard materials. The subsamples taken for trace element analysis were digested in  $\text{HNO}_3$  and analyzed by inductively coupled plasma-atomic emission spectrometer using a PerkinElmer 3100 at

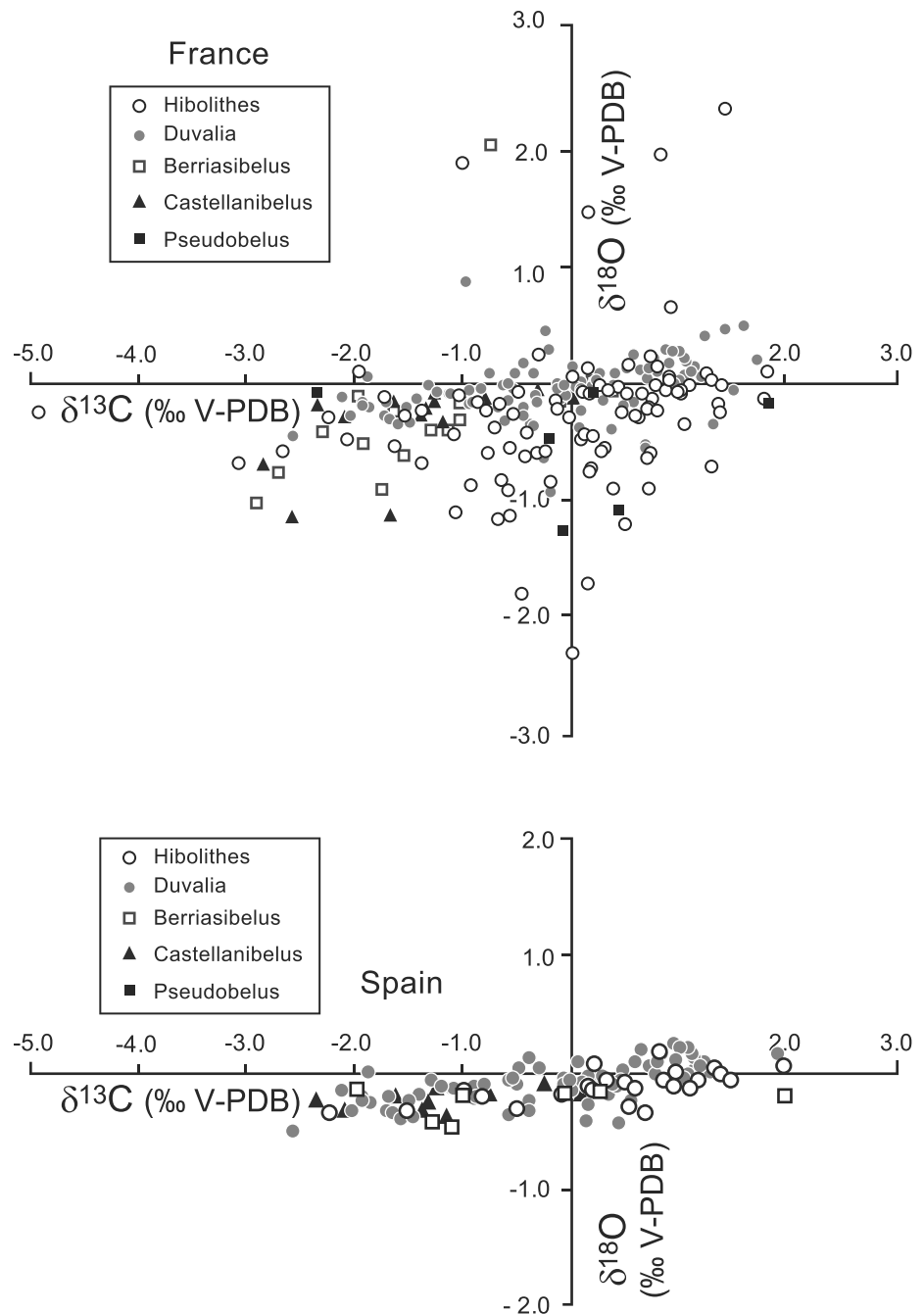


**Figure 4.** Cross plot of  $\delta^{18}\text{O}$  and  $\delta^{13}\text{C}$  data from the belemnites from France and Spain. V-PDB = Vienna Pee Dee Belemnite.

the University of Plymouth. Based upon analysis of duplicate samples reproducibility was better than  $\pm 3\%$  of the measured concentration of each element. Repeat analyses of standards Japanese limestone standard-1 and British Chemical Standard Certified Reference Material 393 were within 2% of the certified values for Sr, Mn, Ca, and Mg and 10% for Fe.

#### 4. Results

Belemnites analyzed from Spain include *Duvalia tornajoensis*, *D. cf. lata constricta*, *D. binervia*, *D. cf. emericii*, *Hibolithes*, *H. cf. jaculoides*, *Berriasibelus*, *Castellanibelus*, and *Pseudobelus*, consistent with earlier studies (e.g., as illustrated in Janssen, 1997, 2003). From France, Valanginian and Hauterivian belemnites include

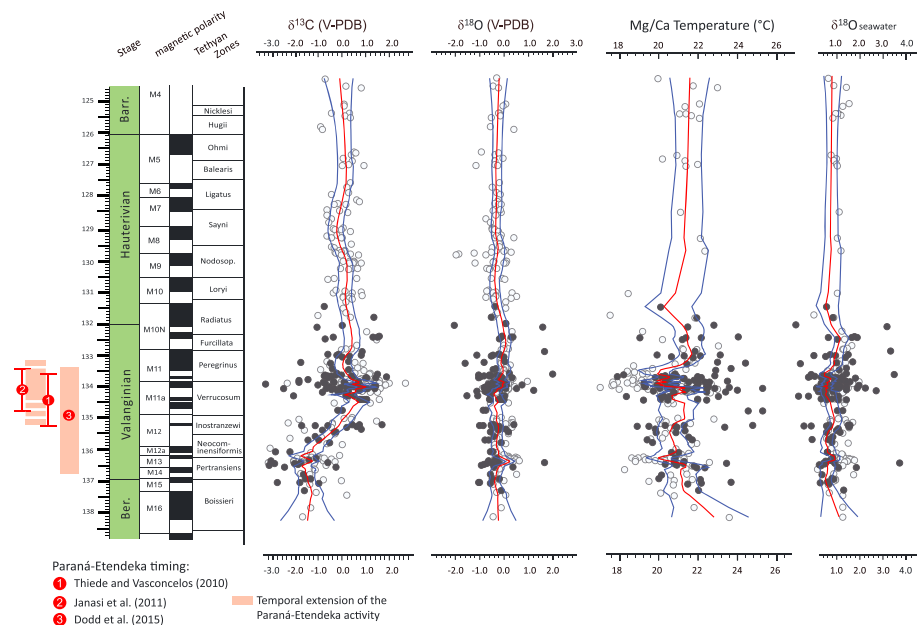


**Figure 5.** Record of oxygen isotopes, carbon isotopes, Mg/Ca temperatures, and  $\delta^{18}\text{O}_{\text{seawater}}$  (with Locally weighted smoothing using the PAST software package (Hammer et al., 2001), through the Valanginian-Hauterivian interval from France plotted against numerical age for the Valanginian-Hauterivian. Blue curves indicate the 95% confidence interval derived using a bootstrap technique. Numerical calibration is modeled on sediment thickness, with adjustments for a variable sedimentation rate. Numerical ages are based on boundary ages of Martinez et al. (2015). Tethyan ammonite zones from Reboulet et al. (2014). The plots incorporate the belemnite isotope and Mg/Ca data of van de Schootbrugge et al. (2000), McArthur et al. (2007), Li et al. (2013), and Bodin et al. (2015), plotted as open circles. V-PDB = Vienna Pee Dee Belemnite.

*Duvalia*, *Hibolithes*, *Berriasibelus*, *Castellanibelus*, and *Pseudobelus*. The belemnite oxygen isotopes (Figure 4 and supporting information data) show only modest variability ranging from  $-0.5\text{‰}$  to  $0.3\text{‰}$  (V-PDB) from Spain and a wider range ( $-4.0\text{‰}$  to  $2.2\text{‰}$ , V-PDB) from France. The carbon isotope values of the belemnites range from  $-2.6\text{‰}$  to  $1.9\text{‰}$  from Spain and  $-4.9\text{‰}$  to  $1.8\text{‰}$  from France. Most belemnites sampled in this study were translucent, although some samples from France exhibited prevalent cloudy and opaque areas particularly around the margins of the rostra and the originally partially porous apical region (Figure 3). These areas tended to be Mn rich as revealed bright orange luminescence. As noted above, such areas were either removed prior to or avoided during subsampling. The determined elemental ranges of belemnite rostra (Table S1 in the supporting information) were as follows: Sr (366–2,898 ppm); Mn (1–851 ppm); Mg (1,624–4,684 ppm); and Fe (21–9,186 ppm). The Ca concentrations ranged from 28.7% to 47.8%. Elemental ranges for Spain and France were very consistent. Further, no tendency for a particular belemnite species to show elevated levels of Fe and/or Mn and hence possibly be more susceptible to diagenetic alteration was noted (Figure 3). In line with other data sets from Spain and France (e.g., Armendáriz et al., 2013; Bodin et al., 2009; van de Schootbrugge et al., 2000) those samples with high Fe and Mn concentrations were considered likely to have undergone some isotopic exchange registered by the precipitation of postdepositional diagenetic calcite and were hence excluded from any further analysis. These high Fe and Mn samples are also typically characterized by low Sr concentrations. Indeed, belemnite samples with low Sr concentrations ( $<800$  ppm) may also suggest some diagenetic alteration (van de Schootbrugge et al., 2000; Wierzbowski et al., 2013) and so were also excluded from any further analysis.

The oxygen isotope data from France fluctuate around  $0.0\text{‰}$  (Figure 5). The most positive values are recorded in the Neocominensiformis Zone, with lighter values seen in the Inostranzewi-Verrucosum and Loryi-Nodosopicatus Zones. Thereafter,  $\delta^{18}\text{O}_{\text{belemnite}}$  values fluctuate around  $-0.4\text{‰}$ . The oxygen isotope data from Spain show a similar pattern with values fluctuating around  $-0.5\text{‰}$  (Figure 6). The most positive values are recorded in the Peregrinus Zone. In terms of carbon, a major positive isotope excursion is evident in the data from France and Spain, beginning in the Inostranzewi ammonite zone and culminating in the Verrucosum Zone (Figures 5 and 6). This excursion reveals a  $3\text{‰}$  change in values and is correlated to the

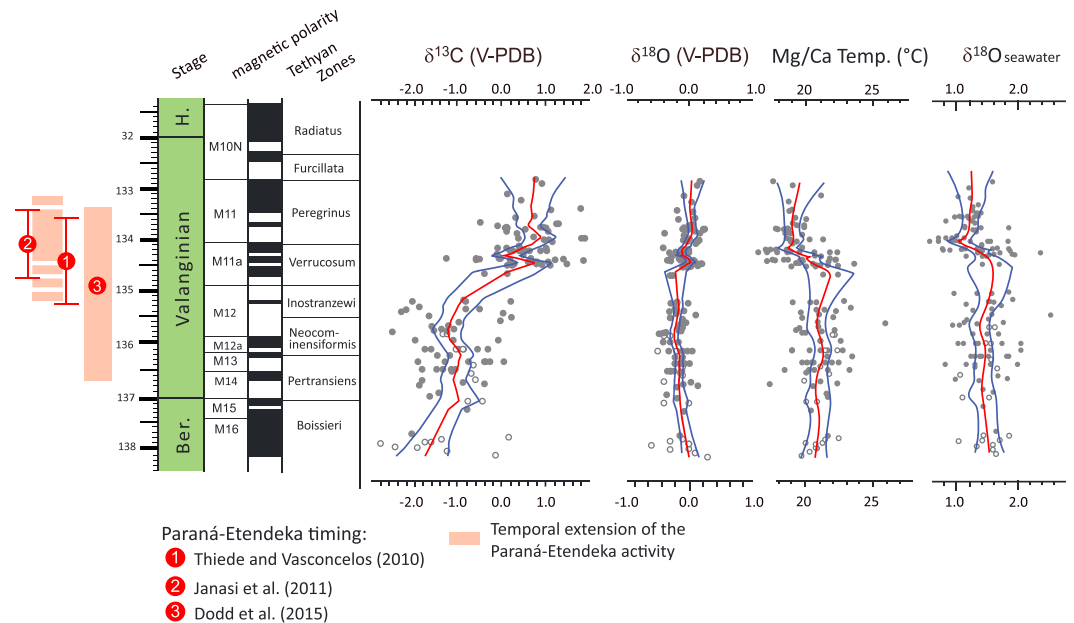


**Figure 6.** Record of oxygen isotopes, carbon isotopes, Mg/Ca temperatures, and  $\delta^{18}\text{O}_{\text{seawater}}$  (with Locally weighted smoothing using the PAST software package (Hammer et al., 2001), through the Valanginian interval from Spain plotted against numerical age for the Valanginian. Blue curves indicate the 95% confidence interval derived using a bootstrap technique. Numerical calibration is modeled on sediment thickness, with adjustments for a variable sedimentation rate. Numerical ages based on using boundary ages of Martinez et al. (2015). Tethyan ammonite zones from Reboulet et al. (2014). The plots incorporate the belemnite isotope and Mg/Ca data of McArthur et al. (2007), plotted as open circles. V-PDB = Vienna Pee Dee Belemnite.

Weissert event (e.g., Erba et al., 2004). Bulk rock data (e.g., Duchamp-Alphonse et al., 2007; Hennig et al., 1999; Kujau et al., 2012; Martinez et al., 2015) likewise show the excursion beginning in the Inostranzewi Zone. Also shown in Figures 5 and 6 are Mg/Ca (mmol/mol) ratio derived paleotemperatures. A difference in mean Mg/Ca between *Duvalia* and *Hibolithes* of 20% is observed. To test if this was a statistical difference, a Student *t* test was conducted. The difference was considered significant at  $P < 0.05$ . Many studies of seawater temperatures and calcitic Mg/Ca ratios (e.g., Klein et al., 1996; Surge & Lohmann, 2008; Vander Putten et al., 2000) have also revealed interspecific differences in temperature sensitivity or related to taxa living at different depths. We therefore minimize this species-specific effect, by using a normalizing approach (e.g., McArthur et al., 2007) whereby we reduced Mg concentrations in *Hibolithes* by 20% (Table S1 reports unadjusted data). Mg/Ca paleotemperatures were calculated here using the equation of Lear et al. (2002) for low Mg calcite (benthic foraminifera) and the calcification constants suggested by Bailey et al. (2003) for belemnites:

$$T(^{\circ}\text{C}) = \ln(\text{MgCa}/1.2)/0.11,$$

(where Mg/Ca is in mmol/mol) which is consistent with other belemnite studies (e.g., McArthur et al., 2007). However, since the biomineralization of Mg/Ca in belemnite calcite cannot be observed or measured, then the paleotemperature values should be treated with caution. Other Mg/Ca temperature equations (e.g., Klein et al., 1996; Surge & Lohmann, 2008) provide different absolute temperatures. For example, applying the Mg/Ca-temperature calibration for the extant oyster *Crassostrea virginica* (Surge & Lohmann, 2008) to our fossil belemnite data results in temperatures that are considerably lower (by ~4–8 °C) than those derived using the equation of Lear et al. (2002). Cretaceous seawater Mg/Ca was likely to be significantly lower compared to modern seawater (e.g., Stanley & Hardie, 1998), and this could also be a significant source of uncertainty and may have led to Cretaceous calcifiers being characterized by lower Mg/Ca ratios. Hence, only Mg/Ca-derived paleotemperature trends (and derived  $\delta^{18}\text{O}_{\text{seawater}}$  trends; see below) can be examined with confidence.

In both France and Spain temperatures using this methodology, modest variability is observed during the Berriasian and earliest Valanginian, and a pronounced cooling event is recorded across the Verrucosum/Peregrinus zonal boundary following the most positive carbon isotope values of the Weissert event. Using the calculated paleotemperatures from Mg/Ca, we then use the equation of Kim and O'Neil (1997) to derive  $\delta^{18}\text{O}_{\text{seawater}}$  (Figures 5 and 6). Utilizing this approach, mean values of the oxygen isotopic composition of seawater from France are calculated to fluctuate around 1.0‰ with more positive values seen within the Neocominensiformis and Furcillata-Loryi Zones. More negative  $\delta^{18}\text{O}_{\text{seawater}}$  values are notable in the Verrucosum Zone. Lighter values are also calculated for the Verrucosum Zone data from Spain.

## 5. Discussion

A major positive carbon isotope excursion is evident in the data from France and Spain, documenting a significant perturbation of the carbon cycle (Figures 5 and 6). A relatively high degree of scatter is also observed. Different belemnite species may have recorded different conditions in the water column, related to differences ecology. However, *Duvalia* and *Hibolites* (the two most commonly encountered species) do show overlapping ranges of carbon isotope values (Figure 4 and Table S1). This suggests a limited species/habitat effect upon carbon isotopes during biomineralization. Alternatively, it might be assumed that some altered samples may not have been identified by the trace element and petrological screening and isotopic outliers result from this. Nevertheless, this carbon isotope excursion appears correlatable to the Weissert event.

The volcanic activity associated with emplacement of the continental Paraná-Etendeka LIP has been considered as a trigger of environmental change associated with the Valanginian Weissert event (e.g., Bajnai et al., 2017; Charbonnier et al., 2017; Duchamp-Alphonse et al., 2007; Erba et al., 2004; Lini et al., 1992; Martinez et al., 2015; Weissert et al., 1998). It might be expected that  $\delta^{13}\text{C}$ -depleted volcanic  $\text{CO}_2$  (with a  $\delta^{13}\text{C}$  of approximately  $-5\text{‰}$ ; Kump & Arthur, 1999) from the Paraná-Etendeka would have resulted in the ocean/atmosphere recording a negative event. This is clearly not the case (Figures 5 and 6), as the Weissert event is characterized by a positive carbon isotope excursion. Notably, the much larger Siberian Trap volcanism, which straddles the Permian-Triassic boundary (e.g., Reichow et al., 2002), is associated with a prominent negative carbon-isotope excursion, but volcanic  $\text{CO}_2$  is also unlikely to have been a main cause of the negative excursion (Kump & Arthur, 1999). A reevaluation of the timing of the onset of the Weissert event is ascertained to be  $135.22 \pm 1$  Ma derived from U-Pb ages from tuff layers in the Neuquén Basin (Aguirre-Urreta et al., 2015) and an update of the Valanginian-Hauterivian astrochronological time scale (Martinez et al., 2015). Therefore, the Valanginian Weissert event appears to have coincided with the onset of the eruptive phase of the Paraná-Etendeka, which has recently been dated between  $134.6 \pm 0.6$  Ma and  $134.3 \pm 0.8$  Ma (Janasi et al., 2011; Thiede & Vasconcelos, 2010). Charbonnier et al. (2017) also show mercury enrichments linked to Valanginian volcanism within the Pertransiens-Inostranzewi Zones. Dodd et al. (2015) recently presented a detailed magnetostratigraphy for the Etendeka portion of the province that suggested emplacement took place a little earlier during Chron 15 (Figures 5 and 6) and suggest a minimum period of volcanic activity in excess of 4 Myr.

The volcanism of the Paraná-Etendeka presumably increased atmospheric  $\text{CO}_2$ , which in turn should elicit a warming. The oxygen isotope values from both Spain and France show very little response to the coincident Paraná-Etendeka LIP (Figures 5 and 6). Either the anticipated warming is erroneous or that the oxygen isotope values are not recording the warming and other factors such as the isotopic composition of seawater is compromising the projected oxygen isotope-derived temperature record. Mg/Ca ratios provide a methodology that is free from the effects of changes in the oxygen isotopic variability of seawater but sensitive to other paleoenvironmental drivers. The Mg/Ca ratio in seawater is spatially constant and unlikely to change on time-scales of less than 1 million years due to the long residence times of both Mg and Ca in the oceans (Broecker & Peng, 1982), although, as noted above, Cretaceous seawater Mg/Ca was likely to be lower than modern seawater (e.g., Stanley & Hardie, 1998). Laboratory culture studies have shown that the pH, carbonate ion concentration, and salinity of seawater act as controls on Mg/Ca ratios in foraminifera but suggest that their influence is small in comparison with temperature (Elderfield et al., 2006; Lea et al., 1999). More recently some studies (e.g., Dueñas-Bohórquez et al., 2009; Ferguson et al., 2008) have suggested that salinity may have had a greater than hitherto expected influence on foraminiferal Mg/Ca ratios. Dueñas-Bohórquez et al.

(2009) suggest that an increase of four salinity units is equivalent to about 1 °C warming, in terms of Mg/Ca ratios. Hence, the changes observed in the Mg/Ca data (Figures 5 and 6) are considered to be temperature related, although a minor contribution from salinity/evaporation cannot be excluded.

The Mg/Ca-derived temperatures from Spain show little variability during the Berriasian and earliest Valanginian. From France, a similar pattern is observed with a cooling event seen during the Neocominensis-formis ammonite zone. A coeval cooling event is not present in Spain and could relate to the lower-resolution data of the Spain section or be a localized event. In both records (Figures 5 and 6) following an interval of warmth, a pronounced cooling event is recorded across the Verrucosum/Peregrinus zonal boundary following the most positive carbon isotope values of the Weissert event. The longer record from France sees a recovery of temperatures during the latest Valanginian and Hauterivian. Hence, unlike other intervals marked by LIP eruptions (e.g., the Ontong Java Plateau, Tejada et al., 2009, or the Caribbean, Kerr, 1998), it is clear from the data presented here that there are no substantial temperature changes (warming) occurring during the main projected phase of the Paraná-Etendeka LIP, despite the large area and volume (approximately equivalent to the Siberian traps,  $1\text{--}2 \times 10^6 \text{ km}^3$ ; Wignall, 2001). It is conjectured that the longer duration of volcanism (4–5 Myr), compared to other LIPs of a similar volume, increased atmospheric and biological recovery time between individual eruptions (Dodd et al., 2015).

A case can be made for cooling in the last stages of the Weissert event (Figures 5 and 6), which possibly reflects substantial CO<sub>2</sub> drawdown. Indeed, increased fertilization of the oceans (e.g., Duchamp-Alphonse et al., 2007; Erba et al., 2004) causing sequestration of marine organic carbon and a consequent decrease (drawdown) of atmospheric CO<sub>2</sub> has been suggested. In the absence of warming and consequent accelerated hydrological cycling (cf. Erba et al., 2004), and the relatively long duration of the eruptive phase of the Paraná-Etendeka, an alternate trigger for increased fertilization of the oceans is implicated. For example, a coupling of cooling, higher dust flux, and increased iron fertilization and productivity has been observed, for example, during the Quaternary (e.g., Martínez-García et al., 2014).

A temperature recovery occurs after the Paraná-Etendeka episode and the Weissert event, to pre-Weissert temperature levels in the latest Valanginian. The inferred cooling coincides with a stable or decrease in the estimated  $\delta^{18}\text{O}_{\text{seawater}}$ . Hence, it is difficult to envisage substantial amounts of ice, as in such circumstances a trend to more positive  $\delta^{18}\text{O}_{\text{seawater}}$  values (globally) would be expected (cf. McArthur et al., 2007). The Valanginian-Hauterivian boundary does see positive  $\delta^{18}\text{O}_{\text{seawater}}$  values, and following the above reasoning,  $\delta^{18}\text{O}_{\text{seawater}}$  values could imply polar ice locking up light oxygen isotopes. However, a cooling trend in the Mg/Ca temperature data is not apparent; hence,  $\delta^{18}\text{O}_{\text{seawater}}$  trend could be related to regional changes (Meissner et al., 2015), such as changes in evaporation or ocean circulation.

## 6. Conclusions

This study evaluates the links between the Paraná-Etendeka volcanism and the Weissert event. Unlike some LIPs, the data presented here indicate that the Paraná-Etendeka did not cause a climate warming (or a mass extinction; Wignall, 2001). The case can be made for cooling in the last stages of the Weissert event, which possibly reflects substantial CO<sub>2</sub> drawdown. In the absence of warming and consequent accelerated hydrological cycling (cf. Erba et al., 2004), and the relatively long duration of the eruptive phase of the Paraná-Etendeka, an alternate trigger for increased fertilization of the oceans is implicated. We interpret the  $\delta^{18}\text{O}_{\text{belemnite}}$  signal as being primarily driven by  $\delta^{18}\text{O}_{\text{seawater}}$  changes and not paleotemperature.

### Acknowledgments

Funding for this research was provided by the Natural Environment Research Council (NERC) Grant awarded to G. D. P. (NE/J020842/1). The data used are listed in the references and supporting information. This paper benefited greatly from two constructive reviews.

### References

- Aguado, R., Company, M., & Tavera, J. M. (2000). The Berriasian-Valanginian boundary in the Mediterranean region: New data from the Caravaca and Cehegín sections, SE Spain. *Cretaceous Research*, 21(1), 1–21. <https://doi.org/10.1006/cres.2000.0198>
- Aguirre-Urreta, B., Lescano, M., Schmitz, M. D., Tunik, M., Concheyro, A., Rawson, P. F., & Ramos, V. A. (2015). Filling the gap: New precise Early Cretaceous radio isotopic ages from the Andes. *Geological Magazine*, 152(03), 557–564. <https://doi.org/10.1017/S001675681400082X>
- Armendáriz, M., Rosales, I., Bádenas, B., Piñuela, L., Aurell, M., & García-Ramos, J. C. (2013). An approach to estimate Lower Jurassic seawater oxygen isotope composition using  $\delta^{18}\text{O}$  and Mg/Ca ratios of belemnite calcites (Early Pliensbachian, northern Spain). *Terra Nova*, 25(6), 439–445. <https://doi.org/10.1111/ter.12054>
- Bailey, T. R., Rosenthal, Y., McArthur, J. M., van de Schootbrugge, B., & Thirlwall, M. F. (2003). Paleooceanographic changes of the Late Pliensbachian–Early Toarcian interval: A possible link to the genesis of an oceanic anoxic event. *Earth and Planetary Science Letters*, 212(3–4), 307–320. [https://doi.org/10.1016/S0012-821X\(03\)00278-4](https://doi.org/10.1016/S0012-821X(03)00278-4)

- Bajnai, D., Palfy, J., Martinez, M., Price, G. D., Nyerges, A., & Fózy, I. (2017). Multi-proxy record of orbital-scale changes in climate and sedimentation during the Weissert event in the Valanginian Bersek Marl Formation (Gerecse Mts., Hungary). *Cretaceous Research*, 75, 45–60. <https://doi.org/10.1016/j.cretres.2017.02.021>
- Barbarin, N., Bonin, A., Mattioli, E., Pucéat, E., Cappetta, H., Gréselle, B., et al. (2012). Evidence for a complex Valanginian nannoconid decline in the Vocontian Basin (south east France). *Marine Micropaleontology*, 84–85, 37–53.
- Bodin, S., Fiet, N., Godet, A., Matera, V., Westermann, S., Clément, A., et al. (2009). Early Cretaceous (latest Berriasian to earliest Aptian) palaeoceanographic change along the northwestern Tethyan margin (Vocontian trough, SE France):  $\delta^{13}\text{C}$ ,  $\delta^{18}\text{O}$  and Sr-isotope belemnite and whole-rock records. *Cretaceous Research*, 30(5), 1247–1262. <https://doi.org/10.1016/j.cretres.2009.06.006>
- Bodin, S., Meissner, P., Janssen, N. M. M., Steuber, T., & Mutterlose, J. (2015). Large igneous provinces and organic carbon burial: Controls on global temperature and continental weathering during the Early Cretaceous. *Global and Planetary Change*, 133, 238–253. <https://doi.org/10.1016/j.gloplacha.2015.09.001>
- Broecker, W. S., & Peng, T.-H. (1982). *Tracers in the sea*, (p. 960). Palisades, New York: Eldigio press.
- Bulot, L. G., Thieuloy, J.-P., Blanc, E., & Klein, J. (1993). Le cadre stratigraphique du Valanginien supérieur et de l'Hauterivien du Sud-Est de la France: Définition des biochronozones et caractérisation de nouveaux biohorizons. *Géologie des Alpes*, 68, 13–56.
- Charbonnier, G., Morales, C., Duchamp-Alphonse, S., Westermann, S., Adatte, T., & Föllmi, K. B. (2017). Mercury enrichment indicates volcanic triggering of Valanginian environmental change. *Scientific Reports*. <https://doi.org/10.1038/srep40808>
- Company, M., Sandoval, J., & Tavera, J. M. (2003). Ammonite biostratigraphy of the uppermost Hauterivian in the Betic Cordillera (SE Spain). *Geobios*, 36(6), 685–694. <https://doi.org/10.1016/j.geobios.2002.12.001>
- Company, M., & Tavera, J. M. (1982). Los ammonites del transito Berriasense-Valanginiense en la region de Cehegin (prov. de Murcia, SE de Espana). *Cuadernos de Geologia Iberica*, 8, 651–664.
- Company, M., & Tavera, J. M. (2015). Lower Valanginian ammonite biostratigraphy in the Subbetic Domain (Betic Cordillera, southeastern Spain). *Carnets de Géologie*, 15(8), 71–88. <https://doi.org/10.4267/2042/56745>
- Cotillon, P., Ferry, S., Gaillard, C., Jautée, E., Latreille, G., & Rio, M. (1980). Fluctuations des paramètres du milieu marin dans le domaine Vocontien (France du Sud-Est) au Crétacé inférieur: Mise en évidence par l'étude de formations marno-calcaires alternantes. *Bulletin de la Société Géologique de France*, 22, 735–744.
- Dodd, S. C., MacNiocaill, C., & Muxworthy, A. R. (2015). Long duration (>4 Ma) and steady-state volcanic activity in the Early Cretaceous Paraná-Etendeka large igneous province: New palaeomagnetic data from Namibia. *Earth and Planetary Science Letters*, 414, 16–29. <https://doi.org/10.1016/j.epsl.2015.01.009>
- Duchamp-Alphonse, S., Gardin, S., Fiet, N., Bartolini, A., Blamart, D., & Pagel, M. (2007). Fertilization of the northwestern Tethys (Vocontian basin, SE France) during the Valanginian carbon isotope perturbation: Evidence from calcareous nannofossils and trace element data. *Palaeogeography, Palaeoclimatology, Palaeoecology*, 243(1-2), 132–151. <https://doi.org/10.1016/j.palaeo.2006.07.010>
- Dueñas-Bohórquez, A., da Rocha, R. E., Kuroyanagi, A., Bijma, J., & Reichart, G.-J. (2009). Effect of salinity and seawater calcite saturation state on Mg and Sr incorporation in cultured planktonic foraminifera. *Marine Micropaleontology*, 73(3-4), 178–189. <https://doi.org/10.1016/j.marmicro.2009.09.002>
- Elderfield, H., Yu, J., Anand, P., Kiefer, T., & Nyland, B. (2006). Calibrations for benthic foraminiferal Mg/Ca paleothermometry and the carbonate ion hypothesis. *Earth and Planetary Science Letters*, 250(3-4), 633–649. <https://doi.org/10.1016/j.epsl.2006.07.041>
- Erba, E., Bartolini, A., & Larson, R. L. (2004). Valanginian Weissert oceanic anoxic event. *Geology*, 32(2), 149–152. <https://doi.org/10.1130/G20008.1>
- Ferguson, J. E., Henderson, G. M., Kucera, M., & Rickaby, R. E. M. (2008). Systematic change of foraminiferal Mg/Ca ratios across a strong salinity gradient. *Earth and Planetary Science Letters*, 265(1-2), 153–166. <https://doi.org/10.1016/j.epsl.2007.10.011>
- Föllmi, K. B., Godet, A., Bodin, S., & Linder, P. (2006). Interactions between environmental change and shallow-water carbonate build-up along the northern Tethyan margin and their impact on the Early Cretaceous carbon-isotope record. *Paleoceanography*, 21, PA4211. <https://doi.org/10.1029/2006PA001313>
- Gardin, S. (2008). Chapter 3. The nannofossil succession of La Charte across the Valanginian-Hauterivian boundary. In E. Mattioli (Ed.), 12th Meeting of the International Nannoplankton Association (Lyon, September 7–10, 2008): Guidebook for the post-congress fieldtrip in the Vocontian Basin, SE France (September 11–13, 2008) *Notebooks on geology* (pp. 11–13). Brest, France: International Nannoplankton Association.
- Giraud, F., Beaufort, L., & Cotillon, P. (1995). Periodicities of carbonate cycles in the Valanginian of the Vocontian trough: A strong obliquity signal. In M. R. House & A. S. Gale (Eds.), *Orbital forcing time scales and cyclostratigraphy*, *Geol. Soc. Spec. Publ.*, (Vol. 85, pp. 143–164). London, UK: Geological Society of London.
- Gradstein, F. M., Ogg, J. G., Schmitz, M. D., & Ogg, G. M. (2012). *The geologic time scale 2012* (1144 pp.). Oxford: Elsevier.
- Gréselle, B., & Pittet, B. (2010). Sea-level reconstructions from the Peri-Vocontian Zone (south-east France) point to Valanginian glacio-eustasy. *Sedimentology*, 57(7), 1640–1684. <https://doi.org/10.1111/j.1365-3091.2010.01159.x>
- Gréselle, B., Pittet, B., Mattioli, E., Joachimski, M., Barbarin, N., Riquier, L., et al. (2011). The Valanginian isotope event: A complex suite of palaeoenvironmental perturbations. *Palaeogeography Palaeoclimatology Palaeoecology*, 306(1-2), 41–57. <https://doi.org/10.1016/j.palaeo.2011.03.027>
- Gröcke, D. R., Price, G. D., Robinson, S. A., Baraboshkin, E. Y., Mutterlose, J., & Ruffell, A. H. (2005). The Upper Valanginian (Early Cretaceous) positive carbon-isotope event recorded in terrestrial plants. *Earth and Planetary Science Letters*, 240(2), 495–509. <https://doi.org/10.1016/j.epsl.2005.09.001>
- Hammer, Ø., Harper, D. A. T., & Ryan, P. D. (2001). Past: Paleontological statistics software package for education and data analysis. *Palaeontologia Electronica*, 4(1), 9. [http://palaeo-electronica.org/2001\\_1/past/issue1\\_01.htm](http://palaeo-electronica.org/2001_1/past/issue1_01.htm)
- Hennig, S., Weissert, H., & Bulot, L. (1999). C-isotope stratigraphy, a calibration tool between ammonite- and magnetostratigraphy: The Valanginian-Hauterivian transition. *Geologica Carpathica*, 50, 91–96.
- Hoedemaeker, P. J., & Leereveld, H. (1995). Biostratigraphy and sequence stratigraphy of the Berriasian–Lowest Aptian (Lower Cretaceous) of the Rio Argos succession, Caravaca, SE Spain. *Cretaceous Research*, 16(2-3), 195–230. <https://doi.org/10.1006/cres.1995.1016>
- Huang, Z., Gradstein, F., & Ogg, J. (1993). A quantitative study of Lower Cretaceous cyclic sequences from the Atlantic Ocean and the Vocontian Basin (SE France). *Paleoceanography*, 8(2), 275–291. <https://doi.org/10.1029/93PA00253>
- Janasi, V. A., de Freitas, V. A., & Heaman, L. H. (2011). The onset of flood basalt volcanism, Northern Paraná, Brazil: A precise U–Pb baddeleyite/zircon age for a Chapecó-type dacite. *Earth and Planetary Science Letters*, 302(1-2), 147–153. <https://doi.org/10.1016/j.epsl.2010.12.005>
- Janssen, N. M. M. (1997). Mediterranean Neocomian belemnites, Part I: Río Argos sequence (province of Murcia, Spain): The Berriasian-Valanginian and the Hauterivian-Barremian boundaries. *Scripta Geologica*, 114, 1–55.

- Janssen, N. M. M. (2003). Mediterranean Neocomian belemnites, Part 2: The Berriasian-Valanginian boundary in southeast Spain (Río Argos, Cañada Lengua and Tornajo). *Scripta Geologica*, 126, 121–183.
- Kemper, E. (1987). Das Klima der Kreide-zeit. *Geologisches Jahrbuch Reihe A*, 96, 5–185.
- Kerr, A. C. (1998). Oceanic plateau formation: A cause of mass extinction and black shale deposition around the Cenomanian–Turonian boundary. *Journal of the Geological Society, London*, 155(4), 619–626. <https://doi.org/10.1144/gsjgs.155.4.0619>
- Kim, S.-T., & O'Neil, J. R. (1997). Equilibrium and nonequilibrium oxygen isotope effects in synthetic carbonates. *Geochimica et Cosmochimica Acta*, 61(16), 3461–3475. [https://doi.org/10.1016/S0016-7037\(97\)00169-5](https://doi.org/10.1016/S0016-7037(97)00169-5)
- Klein, R., Lohmann, K., & Thayer, C. (1996). Bivalve skeletons record sea-surface temperature and  $\delta^{18}\text{O}$  via Mg/Ca and  $^{18}\text{O}/^{16}\text{O}$  ratios. *Geology*, 24(5), 415–418. [https://doi.org/10.1130/0091-7613\(1996\)024<0415:BSRSST>2.3.CO;2](https://doi.org/10.1130/0091-7613(1996)024<0415:BSRSST>2.3.CO;2)
- Kujau, A., Heimhofer, U., Ostertag-Henning, C., Gréselle, B., & Mutterlose, J. (2012). No evidence for anoxia during the Valanginian carbon isotope event—An organic geochemical study from the Vocontian Basin, SE France. *Global and Planetary Change*, 92–93, 92–104.
- Kump, L. R., & Arthur, M. A. (1999). Interpreting carbon-isotope excursions: Carbonates and organic matter. *Chemical Geology*, 161(1–3), 181–198. [https://doi.org/10.1016/S0009-2541\(99\)00086-8](https://doi.org/10.1016/S0009-2541(99)00086-8)
- Lea, D. W., Mashiotta, T., & Spero, H. (1999). Controls on magnesium and strontium uptake in planktonic foraminifera determined by live culturing. *Geochimica et Cosmochimica Acta*, 63(16), 2369–2379. [https://doi.org/10.1016/S0016-7037\(99\)00197-0](https://doi.org/10.1016/S0016-7037(99)00197-0)
- Lear, C. H., Rosenthal, Y., & Slowey, N. (2002). Benthic foraminiferal Mg/Ca-paleothermometry: A revised core-top calibration. *Geochimica et Cosmochimica Acta*, 66(19), 3375–3387. [https://doi.org/10.1016/S0016-7037\(02\)00941-9](https://doi.org/10.1016/S0016-7037(02)00941-9)
- Li, Q., McArthur, J. M., Doyle, P., Janssen, N., Leng, M. J., Muller, W., & Reboulet, S. (2013). Evaluating Mg/Ca in belemnite calcite as a palaeo-proxy. *Palaeogeography Palaeoclimatology Palaeoecology*, 388, 98–108. <https://doi.org/10.1016/j.palaeo.2013.07.030>
- Lini, A., Weissert, H., & Erba, E. (1992). The Valanginian carbon isotope event: A first episode of greenhouse climate conditions during the Cretaceous. *Terra Nova*, 4(3), 374–384. <https://doi.org/10.1111/j.1365-3121.1992.tb00826.x>
- Martin-Algarra, A., Ruiz-Ortiz, P. A., & Vera, J. A. (1992). Factors controlling Cretaceous turbidite deposition in the Betic Cordillera. *Revista de la Sociedad Geológica de España*, 5, 53–80.
- Martinez, M., Deconinck, J.-F., Pellenard, P., Riquier, L., Company, M., Reboulet, S., & Moiroud, M. (2015). Astrochronology of the Valanginian-Hauterivian stages (Early Cretaceous): Chronological relationships between the Paraná-Etendeka large igneous province and the Weissert and the Faraoni events. *Global and Planetary Change*, 131, 158–173.
- Martinez, M., Pellenard, P., Deconinck, J.-F., Monna, F., Riquier, L., Boulila, S., et al. (2012). An orbital floating time scale of the Hauterivian/Barremian GSSP from a magnetic susceptibility signal (Río Argos, Spain). *Cretaceous Research*, 36, 106–115.
- Martínez-García, A., Sigman, D. M., Ren, H., Anderson, R. F., Straub, M., Hodell, D. A., et al. (2014). Iron fertilization of the Subantarctic Ocean during the Last Ice Age. *Science*, 343(6177), 1347–1350. <https://doi.org/10.1126/science.1246848>
- Masse, J. P., Bellion, Y., Benkheilil, J., Ricou, L. E., Dercourt, J., & Guiraud, R. (1993). Early Aptian (114 to 111 Ma). In J. Dercourt, L. E. Ricou, & B. Vrielynck (Eds.), *Atlas, Tethys, palaeoenvironmental maps* (pp. 135–152). Paris: Gauthier-Villars.
- McArthur, J. M., Janssen, N. M. M., Reboulet, S., Leng, M. J., Thirlwall, M. F., & Van de Schootbrugge, B. (2007). Palaeo-temperatures, polar ice-volume, and isotope stratigraphy (Mg/Ca,  $\delta^{18}\text{O}$ ,  $\delta^{13}\text{C}$ ,  $^{87}\text{Sr}/^{86}\text{Sr}$ ): The Early Cretaceous (Berriasian, Valanginian, Hauterivian). *Palaeogeography Palaeoclimatology Palaeoecology*, 248(3–4), 391–430. <https://doi.org/10.1016/j.palaeo.2006.12.015>
- McArthur, J. M., Mutterlose, J., Price, G. D., Rawson, P. F., Ruffell, A., & Thirlwall, M. F. (2004). Belemnites of Valanginian, Hauterivian and Barremian age: Sr-isotope stratigraphy, composition ( $^{87}\text{Sr}/^{86}\text{Sr}$ ,  $\delta^{13}\text{C}$ ,  $\delta^{18}\text{O}$ , Na, Sr, Mg), and palaeo-oceanography. *Palaeogeography Palaeoclimatology Palaeoecology*, 202(3–4), 253–272. [https://doi.org/10.1016/S0031-0182\(03\)00638-2](https://doi.org/10.1016/S0031-0182(03)00638-2)
- Meissner, P., Mutterlose, J., & Bodin, S. (2015). Latitudinal temperature trends in the Northern Hemisphere during the Early Cretaceous (Valanginian-Hauterivian). *Palaeogeography, Palaeoclimatology, Palaeoecology*, 424, 17–39. <https://doi.org/10.1016/j.palaeo.2015.02.003>
- Melinte, M., & Mutterlose, J. (2001). A Valanginian (Early Cretaceous) “boreal nannoplankton excursion” in sections from Romania. *Marine Micropaleontology*, 43(1–2), 1–25. [https://doi.org/10.1016/S0377-8398\(01\)00022-6](https://doi.org/10.1016/S0377-8398(01)00022-6)
- Mutterlose, J. (1992). Migration and evolution patterns of floras and faunas in marine Early Cretaceous sediments of NW Europe. *Palaeogeography Palaeoclimatology Palaeoecology*, 94(1–4), 261–282. [https://doi.org/10.1016/0031-0182\(92\)90123-M](https://doi.org/10.1016/0031-0182(92)90123-M)
- Price, G. D. (1999). The evidence and implications of polar ice during the Mesozoic. *Earth-Science Reviews*, 48(3), 183–210. [https://doi.org/10.1016/S0012-8252\(99\)00048-3](https://doi.org/10.1016/S0012-8252(99)00048-3)
- Price, G. D., & Passey, B. H. (2013). Dynamic polar climates in a greenhouse world: Evidence from clumped isotope thermometry of Early Cretaceous belemnites. *Geology*, 41(8), 923–926. <https://doi.org/10.1130/G34484.1>
- Pucéat, E., Lécuyer, C., Sheppard, S. M. F., Dromart, G., Reboulet, S., & Grandjean, P. (2003). Thermal evolution of Cretaceous Tethyan marine waters inferred from oxygen isotope composition of fish tooth enamels. *Paleoceanography*, 18(2), 1029. <https://doi.org/10.1029/2002PA000823>
- Reboulet, S., & Atrops, F. (1995). Rôle du climat sur les migrations et la composition des peuplements d'ammonites du Valanginien supérieur du bassin Vocontien (S–E de la France). *Geobios*, 18, 357–365.
- Reboulet, S., & Atrops, F. (1997). Quantitative variations of the Valanginian ammonite fauna of the Vocontian Basin (south-eastern France) between limestone-marls and within parasequences. *Palaeogeography, Palaeoclimatology, Palaeoecology*, 135(1–4), 145–155. [https://doi.org/10.1016/S0031-0182\(97\)00023-0](https://doi.org/10.1016/S0031-0182(97)00023-0)
- Reboulet, S., Atrops, F., Ferry, S., & Schaaf, A. (1992). Renouveau des ammonites en fosse Vocontienne a la limite Valanginien-Hauterivien. *Geobios*, 25, 469–476.
- Reboulet, S., Mattioli, E., Pittet, B., Baudin, F., Olivero, D., & Proux, O. (2003). Ammonoid and nannoplankton abundance in Valanginian (Early Cretaceous) limestone–marl successions from the Southeast France Basin: Carbonate dilution or productivity? *Palaeogeography, Palaeoclimatology, Palaeoecology*, 201(1–2), 113–139. [https://doi.org/10.1016/S0031-0182\(03\)00541-8](https://doi.org/10.1016/S0031-0182(03)00541-8)
- Reboulet, S., Szives, O., Aguirre-Urreta, B., Barragán, R., Company, M., Idakieva, V., et al. (2014). Report on the 5th International Meeting of the IUGS Lower Cretaceous Ammonite Working Group, the Kilian Group (Ankara, Turkey, 31st August 2013). *Cretaceous Research*, 50, 126–137.
- Reichow, M. K., Saunders, A. D., White, R. V., Pringle, M. S., Al'Mukhamedov, A. I., Medvedev, A., & Korda, N. (2002). New  $^{40}\text{Ar}$ – $^{39}\text{Ar}$  data on basalts from the West Siberian Basin: Extent of the Siberian flood basalt province doubled. *Science*, 296(5574), 1846–1849. <https://doi.org/10.1126/science.1071671>
- Sprenger, A., & Ten Kate, W. G. (1993). Orbital forcing of calcilutite-marl cycles in southeast Spain and an estimate for the duration of the Berriasian Stage. *Geological Society of America Bulletin*, 105(6), 807–818. [https://doi.org/10.1130/0016-7606\(1993\)105<0807:OFOCMC>2.3.CO;2](https://doi.org/10.1130/0016-7606(1993)105<0807:OFOCMC>2.3.CO;2)
- Stanley, S., & Hardie, L. (1998). Secular oscillations in the carbonate mineralogy of reef-building and sediment-producing organisms driven by tectonically forced shifts in seawater chemistry. *Palaeogeography, Palaeoclimatology, Palaeoecology*, 144(1–2), 3–19. [https://doi.org/10.1016/S0031-0182\(98\)00109-6](https://doi.org/10.1016/S0031-0182(98)00109-6)

- Surge, D., & Lohmann, K. (2008). Evaluating Mg/Ca ratios as a temperature proxy in the estuarine oyster, *Crassostrea virginica*. *Journal of Geophysical Research*, 113, G02001. <https://doi.org/10.1029/2007JG000623>
- Tejada, M. L. G., Suzuki, K., Kuroda, J., Coccioni, R., Mahoney, J. J., Ohkouchi, N., et al. (2009). Ontong Java Plateau eruption as a trigger for the early Aptian oceanic anoxic event. *Geology*, 37(9), 855–858. <https://doi.org/10.1130/G25763A.1>
- Thiede, D. S., & Vasconcelos, P. M. (2010). Paraná flood basalts: Rapid extrusion hypothesis confirmed by new  $^{40}\text{Ar}/^{39}\text{Ar}$  results. *Geology*, 38(8), 747–750. <https://doi.org/10.1130/G30919.1>
- van de Schootbrugge, B., Föllmi, K. B., Bulot, L. G., & Burns, S. J. (2000). Paleoclimatographic changes during the Early Cretaceous (Valanginian-Hauterivian): Evidence from oxygen and carbon stable isotopes. *Earth and Planetary Science Letters*, 290(181), 15–31.
- Vander Putten, E., Dehairs, F., Keppens, E., & Baeyens, W. (2000). High resolution distribution of trace elements in the calcite shell layer of modern *Mytilus edulis*: Environmental and biological controls. *Geochimica et Cosmochimica Acta*, 64(6), 997–1011. [https://doi.org/10.1016/S0016-7037\(99\)00380-4](https://doi.org/10.1016/S0016-7037(99)00380-4)
- Weissert, H., Lini, A., Föllmi, K. B., & Kuhn, O. (1998). Correlation of Early Cretaceous carbon isotope stratigraphy and platform drowning events: A possible link? *Palaeogeography, Palaeoclimatology, Palaeoecology*, 137(3–4), 189–203. [https://doi.org/10.1016/S0031-0182\(97\)00109-0](https://doi.org/10.1016/S0031-0182(97)00109-0)
- Wierzbowski, H., Rogov, M. A., Matyja, B. A., Kiselev, D., & Ippolitov, A. (2013). Middle-Upper Jurassic (Upper Callovian-Lower Kimmeridgian) stable isotope and elemental records of the Russian Platform: Indices of oceanographic and climatic changes. *Global and Planetary Change*, 107, 196–212. <https://doi.org/10.1016/j.gloplacha.2013.05.011>
- Wignall, P. B. (2001). Large igneous provinces and mass extinctions. *Earth-Science Reviews*, 53(1–2), 1–33. [https://doi.org/10.1016/S0012-8252\(00\)00037-4](https://doi.org/10.1016/S0012-8252(00)00037-4)